Structural Engineering and Mechanics, *Vol. 75, No. 1 (2020) 109-122*
DOI: https://doi.org/10.12989/sem.2020.75.1.109

Static analysis of multiple graphene sheet systems in cylindrical bending and resting on an elastic medium

Chih-Ping Wu* and Chih-Chen Lin

Department of Civil Engineering, National Cheng Kung University, Taiwan, Republic of China

(Received September 12, 2018, Revised April 5, 2019, Accepted February 8, 2020)

Abstract. An asymptotic local plane strain elasticity theory is reformulated for the static analysis of a simply-supported, multiple graphene sheet system (MGSS) in cylindrical bending and resting on an elastic medium. The dimension of the MGSS in the y direction is considered to be much greater than those in the x and z directions, such that all the field variables are considered to be independent of the y coordinate. Eringen's nonlocal constitutive relations are used to account for the small length scale effects in the formulation examining the static behavior of the MGSS. The interaction between the MGSS and its surrounding foundation is modelled as a Winkler foundation with the parameter k_w, and the interaction between adjacent graphene sheets (GSs) is considered using another Winkler model with the parameter c_w. A parametric study with regard to some effects on the static behavior of the MGSS resting on an elastic medium is undertaken, such as the aspect ratio, the number of the GSs, the stiffness of the medium between the adjacent layers and that of the surrounding medium of the MGSS, and the nonlocal parameter.

Keywords: Eringen's nonlocal elasticity theory; foundation; multiple graphene sheet systems; nonlocal plane strain elasticity theory; static; the perturbation method

1. Introduction

In recent decades, carbon nanotubes (CNTs) (Iijima 1991) and graphene sheets (GSs) (Novoselov *et al.* 2004) were discovered in materials science laboratories one after the other. These two nanoscale materials are regarded as the most crucial materials having the potential for applications in advanced engineering due to their excellent mechanical, chemical, thermal, and electrical material properties. With the rapid development of nanoscience and nanotechnology, various relevant applications of these materials have been exploited, including their use in double and multiple GS systems. For example, some nanoscale devices for double or multiple nanoplate systems have been developed, such as nano-resonators and nanoscale mass-sensors (Karličić *et al.* 2015, Rajabi and Hosseini-Hashemi 2017a, b), and the corresponding analytical and numerical models have also been presented (Arani *et al*. 2012, Karličić *et al.* 2016, Khaniki 2018, Murmu and Adhikari 2010). CNTs and GSs have been used to mix with polymer, ceramic or metal materials to form the beam-, plate- and shell-like CNT- and GS-reinforced composite structures (Bakshi *et al.* 2010, Yengejeh *et al.* 2017). The double and multiple nanobeam structures were used to develop the cavity nanooptomechanical system (NOMs) (Metcalfe 2014). The practical applications of NOMs include displacement sensing and on-chip optical data processing (Kippenberg and Vahala 2007). In addition, graphene material is a two-dimensional (2D) sheet of carbon atoms with a hexagonal configuration, which results in its extraordinary properties, such as a very large surface area, a tunable band gap, and high mechanical strength and thermal conductivity, and also gives GS the advantage of potential application in electrochemical sensing and biosensing (Kuila *et al.* 2011, Pumera *et al.* 2010).

As mentioned above, graphene materials have many applications in cutting-edge industries, so development of a definitive theoretical methodology and numerical models to accurately predict their structural behavior has thus attracted considerable attention. Based on Eringen's nonlocal constitutive relations (ENCR) (Eringen, 1972, 2002; Eringen and Edelen, 1972), some 2D local plate theories have been reformulated to investigate the mechanical behavior of single- and multi-layered nanoplates and GSs embedded or non-embedded in an elastic medium. Aghababaei and Reddy (2009) developed Reddy's nonlocal third-order shear deformation theory (TSDT) for the static and free vibration analyses of simply-supported, single-layered nanoplates and GSs, in which Navier's solutions for the stress and displacement components and natural frequency parameters of the GSs were presented. Based on a refined plate theory, Yazid *et al.* (2018) examined the buckling behavior of an orthotropic single-layered GS resting on the Pasternak foundation, in which the shear correction factor was unnecessary. Combining the ENCR and von Kármán geometrical nonlinearity (VKGN), Reddy (2010) investigated the nonlinear bending behavior of single-layered nanoplates using the nonlocal first-order shear deformation theory (FSDT) and the nonlocal classical plate theory (CPT), which were also extended to an analysis of double-layered nanoplates by Pradhan and Phadikar (2009). Some effects on the natural frequency parameters of the nanoplate were

*Corresponding author, Professor
E-mail: cpwu@mail.ncku.edu.tw

http://www.techno-press.com/journals/sem&subpage=7
ISSN: 1225-4568 (Print), 1598-6217 (Online)

studied, including the nonlocal parameter, the aspect ratio, the Young's modulus of the nanoplate, and the stiffness of Winkler foundation effects. Based on the nonlocal CPT, Naderi and Saidi (2014) studied the postbuckling behavior of GSs in a polymer environment, in which the interaction force between adjacent GSs and that between the GSs and their surrounding medium were modelled as the Winkler model with a nonlinear stiffness function of the GS's deflection. Based on the nonlocal CPT, Anjomshoa *et al.* (2014) developed a finite element method for the buckling analysis of multi-layered GSs on an elastic substrate. Naderi and Saidi (2014) developed a modified nonlocal Mindlin plate theory for the stability analysis of nanoplates under either a uniaxial or a biaxial in-plane loading. Sobhy (2017) developed a nonlocal four-unknown shear deformation theory for the coupled hygro-thermo-mechanical vibration and buckling analyses of functionally graded (FG) nanoplates resting on a two-parameter Pasternak foundation, where the material properties of the nanoplate were assumed to obey two exponential function distributions through the thickness direction. Khetir *et al.* (2017) proposed a new nonlocal trigonometric shear deformation theory to study the thermal buckling behavior of FG nanoplates embedded in an elastic medium under different thermal environments. Based on the nonlocal refined sinusoidal shear deformation theory (SSDT), Thai (2012), Thai and Vo (2012), and Thai *et al.* (2014) presented analytical solutions for the bending, buckling, and vibration problems of simply-supported, single-layered nanobeams and nanoplates. In their articles, it was concluded that the small length scale effect and shear deformation have significant effects on the structural behavior of nanostructures as they become thicker. Bessaim *et al.* (2015) reformulated a nonlocal quasi-three-dimensional (3D) trigonometric plate theory for the free vibration analysis of nanoscale plates, and FG nanoplates were also examined by Belkorissat *et al.* (2015), Besseghier *et al.* (2017) and Bounouara *et al.* (2016) using a nonlocal refined four-variable shear deformation theory, a nonlocal trigonometric shear deformation theory, and a zero$^{\text{th}}$-order shear deformation theory, respectively.

Three-dimensional (3D) benchmark solutions for assorted structural analyses of local and nonlocal plates and shells are valuable because they can provide a reference for assessing various 2D local and nonlocal refined/advanced theories. However, these 3D solutions are rare in the open literature due to their mathematical complexity and the fact that they are difficult to solve as compared with those obtained using the 2D theories. Pagano (1969) is a pioneer, who presented the exact 3D solutions for the stress and deformation analyses of laminated composite plates subjected to cylindrical bending-type loading on the top surface of a plate. Consequently, there have been numerous articles with regard to this issue available in the literature (Fahsi *et al.* 2012, Navazi and Haddadpour 2008, Park and Lee 2003, Sayyad *et al*. 2014, She *et al.* 2017). Based on the 3D nonlocal elasticity theory, Jomehzadeh and Saidi (2011) presented a 3D vibration analysis of nanoplates. In their formulation, the basic equations of the 3D nonlocal elasticity theory were decoupled as three equations in terms of the displacement components and another three equations in terms of the rotation components. The Navier method was used to obtain the frequency parameters of nanoplates by solving these two sets of decoupling equations. Within the framework of nonlocal plane strain theory, Wu and Chen (2019) developed a nonlocal asymptotic theory for the cylindrical vibration analysis of multiple GS systems embedded in an elastic medium.

After a close literature survey, it can be found that 3D benchmark solutions for assorted structural analyses of nanoplates and GSs are rare as compared with those for various analyses of their local counterparts. To the best of the authors' knowledge, there is no article examining the cylindrical bending behavior of multiple GS systems. This article is thus aimed toward investigating the current issue using the perturbation method (Nayfeh 1993). The multiple GS system is considered to be infinitely long in the y direction, simply supported at the two edges in the x direction, subjected to the sinusoidal load on the topmost surface of the multiple GS system, and resting on a Winkler foundation. In the formulation, both the interaction effects between adjacent GSs and those between the multiple GS system and its surrounding medium are modelled as Winkler models with different stiffness coefficients, namely c_w and k_w, respectively. The eight basic equations for an individual GS are first reduced into four equations using the direct elimination method. After a series of mathematic manipulations, such as nondimensionalization, asymptotic expansion to the primary field variables, and asymptotic integration through the thickness direction for each basic equation, recursive sets of the governing equations (GEs) of each individual GS can be obtained for various order problems, in which the differential operators of these GEs for various order problems are identical to one another, although with different forms of nonhomogeneous terms. With using the assembly process, the GEs of the multiple GS system for various order problems can be formed. By solving these resulting GEs, the stress and deformation of the GSs constituting the multiple GS system can thus be obtained in a hierarchic and consistent manner, and the solution process applied in the leading order problem can be repeatedly used for the higher-order problems.

2. The asymptotic nonlocal plane strain elasticity theory

2.1 Basic equations

As mentioned above, a simply-supported, N_l-GS system with an infinite length subjected to a cylindrical bending-type load is considered. Figure 1 shows the cross-section of a triple-GS system and the Winkler's models used to describe the interaction effects between the triple-GS system and its surrounding medium as well as those between adjacent GSs, in which a set of Cartesian coordinates (x, y and z_m) is located at the mid-plane of the m^{th}-GS and the thickness and dimension in the x direction for each GS are denoted as H and L_x, respectively.

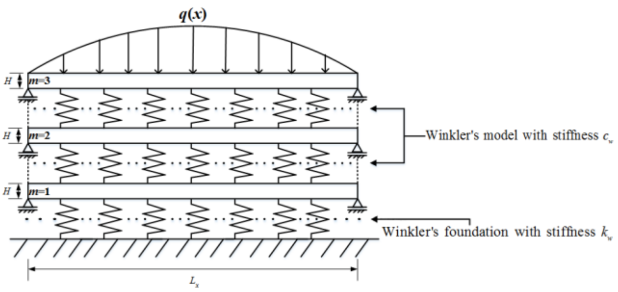

Fig. 1 Configuration, dimensions, and loading conditions of a cross-section of the triple-GS system

According to the ENCR (Eringen 1972, 2002 and Eringen and Edelen 1972), the nonlocal constitutive behavior of a Hookean solid can be written as

$$\sigma_{ij}(\mathbf{x}) = \int \alpha\left(\|\mathbf{x}-\mathbf{x}'\|,\ \tau\right) C_{ijkl}\ \varepsilon_{kl}(\mathbf{x}')dV(\mathbf{x}'), \qquad \forall \mathbf{x} \in V \tag{1}$$

where the elastic modulus tensor of classical isotropic elasticity is defined as C_{ijkl}, and σ_{ij} and ε_{kl} denote the stress and strain components, respectively. The nonlocal modulus or attenuation function, which incorporates the constitutive equations into the nonlocal effect at the reference point $\mathbf{x}$ produced by local strain at the source $\mathbf{x}'$, is defined as $\alpha(\|\mathbf{x}-\mathbf{x}'\|, \tau)$, in which the symbol $\|\mathbf{x}-\mathbf{x}'\|$ is the Euclidean distance. $\tau = e_0 a/l$, in which e_0 is a constant appropriate to each material, a is an internal characteristic length (e.g., length of C-C bond, lattice parameter, or granular distance), and l is an external characteristic length (e.g., crack length or wavelength).

For the sake of convenience of computation, the integral-partial differential equations of Eq. (1) are transformed to the singular partial differential equations of a special class of physically admissible kernels, as follows:

$$\left(1-\mu\nabla^2\right)\sigma_{ij} = C_{ijkl}\varepsilon_{kl} \tag{2}$$

where μ is the nonlocal parameter, and $\mu = (e_0 a)^2$. ∇^2 is the Laplacian operator, in which $\nabla^2 = (\partial_{xx} + \partial_{zz})$ is used for the current nonlocal plane strain problem.

According to Eringen's elasticity theory, the linear constitutive equations valid for the symmetrical class of elastic materials for a plane strain problem are given by

$$\left(1-\mu\nabla^2\right)\begin{Bmatrix}\sigma_{xm}\\ \sigma_{zm}\\ \tau_{xzm}\end{Bmatrix} = \begin{bmatrix} c_{11} & c_{13} & 0\\ c_{13} & c_{33} & 0\\ 0 & 0 & c_{55}\end{bmatrix}\begin{Bmatrix}\varepsilon_{xm}\\ \varepsilon_{zm}\\ \gamma_{xzm}\end{Bmatrix} \tag{3}$$

where ε_{xm}, ε_{zm}, and γ_{xzm} denote the strain components induced in the m^{th}-GS. σ^l_{xm}, σ^l_{zm} and τ^l_{xzm} as well as σ_{xm}, σ_{zm} and τ_{xzm} are defined as the local and nonlocal stress components induced in the m^{th}-GS, respectively, in which $(\sigma^l_{xm},\ \sigma^l_{zm},\ \tau^l_{xzm}) = (1-\mu\nabla^2)(\sigma_{xm},\ \sigma_{zm},\ \tau_{xzm})$. c_{ij} (i, j=1, 3 and 5) are the elastic coefficients relative to the geometrical axes of the GS system. For an isotropic material GS system the coefficients c_{ij} will be reduced to $c_{11} = c_{33} = [(1-\upsilon)E/(1+\upsilon)(1-2\upsilon)], c_{13} = [\upsilon E/(1+\upsilon)(1-2\upsilon)]$, and $c_{55} = \left[E/2(1+\upsilon)\right]$, in which E and υ are the Young's modulus and Poisson's ratio, respectively.

The nonzero strain components of the m^{th}-GS in terms of the displacement components are

$$\varepsilon_{xm} = \frac{\partial u_{xm}}{\partial x}, \quad \varepsilon_{zm} = \frac{\partial u_{zm}}{\partial z_m}, \quad \gamma_{xzm} = \frac{\partial u_{xm}}{\partial z_m} + \frac{\partial u_{zm}}{\partial x} \tag{4a-c}$$

where u_{xm} and u_{zm} are the displacement components induced in the m^{th}-GS.

The stress equilibrium equations of an elastic body without accounting for body forces for the m^{th}-GS are given by

$$\frac{\partial\sigma_{xm}}{\partial x} + \frac{\partial\tau_{xzm}}{\partial z_m} = 0 \tag{5}$$

$$\frac{\partial\tau_{xzm}}{\partial x} + \frac{\partial\sigma_{zm}}{\partial z_m} = 0 \tag{6}$$

The boundary conditions of the problem are specified, as follows:

On the top and bottom surfaces of the m^{th}-GS, the transverse loads are given by

$$\begin{bmatrix}\tau_{xzm} & \sigma_{zm}\end{bmatrix} = \begin{bmatrix}0 & \bar{q}^{\pm}_{zm}\end{bmatrix} \text{ on } z_m = \pm h \tag{7}$$

where h denotes one-half of the total thickness (H) of the m^{th}-GS. The positive directions of $\bar{q}^{+}_{zm}$ and $\bar{q}^{-}_{zm}$ are defined to be upward and downward, respectively, and $\bar{q}^{+}_{zm} = c_w(\bar{u}_{z(m+1)} - \bar{u}_{zm})$ when m=1-(N_l-1) and $\bar{q}^{-}_{zm} = c_w(\bar{u}_{zm} - \bar{u}_{z(m-1)})$ when m=2-N_l, $\bar{q}^{+}_{zN_l} = -\bar{q}_z(x)$ and $\bar{q}^{-}_{z1} = k_w\,\bar{u}_{z1}$, in which k_w is the Winkler stiffness of the surrounding elastic medium, respectively, and c_w is that of the medium between adjacent GSs. $\bar{q}_z(x)$ is the applied external load, the positive direction of which is defined to be downward, and $\bar{u}_{zm}$ denotes the out-of-plane displacement component at the mid-plane of the m^{th}-GS layer.

The edge boundary conditions of the m^{th}-GS are considered as simply-supported edges, and are given as follows:

At the edges (x=0 and x=L_x), the boundary conditions are

$$\sigma_{xm} = u_{zm} = 0 \tag{8}$$

Equations (3)-(6) represent 8 basic equations of each individual GS for the nonlocal plane strain problem.

2.2 Nondimensionalization

A set of dimensionless coordinates and elastic field variables is defined, as follows:

$$x_1 = x/L,\quad x_3 = z_m/(L\in),\quad u_{1m} = u_{xm}/(L\in),$$
$$u_{3m} = u_{zm}/L,\quad \sigma_{1m} = \sigma_{xm}/(Q\in),$$
$$\tau_{13m} = \tau_{xzm}/\left(Q\in^2\right),\quad \sigma_{3m} = \sigma_{zm}/\left(Q\in^3\right), \tag{9a-i}$$
$$\bar{\mu}_1 = \mu/L^2,\quad \bar{\mu}_2 = \mu/\left(L^2\in^4\right)$$

where $\in = h/L$. L and Q denote the reference length and elastic modulus, and these are given as $L = L_x$ and $Q=E$ in this work.

In order to make the formulation suitable for mathematical treatment, the authors eliminate the in-plane stress (σ_{xm}) and strain ($\varepsilon_{xm}, \varepsilon_{zm}, \gamma_{xzm}$) components from Eqs. (3)-(6), introduce Eq. (9) in the resulting equations, and then express the basic equations in terms of the dimensionless forms of displacement (u_{1m}, u_{3m}) and transverse stress (τ_{13m}, σ_{3m}) components, as follows:

$$\begin{aligned} u_{3m},_3 = &-\in^2 \tilde{c}_{13}\, u_{1m,1} + \in^4 \tilde{c}_{33}^{-1} \left[1-\bar{\mu}_1 \partial_{11}\right]\sigma_{3m} \\ &+ \in^6 \tilde{c}_{33}^{-1} \left(-\bar{\mu}_2 \partial_{33}\right) \sigma_{3m} \end{aligned} \tag{10}$$

$$\begin{aligned} u_{1m},_3 = &-u_{3m},_1 + \in^2 \tilde{c}_{55}^{-1} \left[1-\bar{\mu}_1 \partial_{11}\right]\tau_{13m} \\ &+ \in^4 \tilde{c}_{55}^{-1} \left(-\bar{\mu}_2 \partial_{33}\right)\tau_{13m} \end{aligned} \tag{11}$$

$$\begin{aligned} \left[\left(1-\bar{\mu}_1 \partial_{11}\right)\tau_{13m}\right],_3 = &-\tilde{Q}_{11}\, u_{1m},_{11} + \in^2 \left[\left(\bar{\mu}_2 \partial_{33}\right)\tau_{13m}\right],_3 \\ &-\in^2 \tilde{c}_{13} \left[\left(1-\bar{\mu}_1 \partial_{11}\right)\sigma_{3m}\right],_1 - \in^4 \tilde{c}_{13}\left[\left(-\bar{\mu}_2 \partial_{33}\right)\sigma_{3m}\right],_1, \end{aligned} \tag{12}$$

$$\left[\left(1-\bar{\mu}_1 \partial_{11}\right)\sigma_{3m}\right],_3 = -\left[\left(1-\bar{\mu}_1 \partial_{11}\right)\tau_{13m}\right],_1 \tag{13}$$

where

$$\tilde{c}_{i3} = c_{i3}/c_{33} \quad (i = 1 \text{ and } 2), \quad \tilde{c}_{kk} = c_{kk}/Q \quad (k = 3 \text{ and } 5),$$
$$\tilde{Q}_{ij} = Q_{ij}/Q, \quad Q_{ij} = c_{ij} - \left(c_{i3}\, c_{j3}/c_{33}\right) \quad (i,\, j = 1 \text{ and } 3).$$

Following a similar derivation process, the authors rewrite the in-surface stresses in the dimensionless form, as follows:

$$\begin{aligned} \left(1-\bar{\mu}_1 \partial_{11}\right)\sigma_{1m} = &\ \tilde{Q}_{11}\, u_{1m},_1 + \in^2 \left(\bar{\mu}_2 \partial_{33}\right) \sigma_{1m} \\ &+ \in^2 \tilde{c}_{13} \left(1-\bar{\mu}_1 \partial_{11}\right)\sigma_{3m} - \in^4 \tilde{c}_{13} \left(\bar{\mu}_2 \partial_{33}\right)\sigma_{3m} \end{aligned} \tag{14}$$

The dimensionless forms of the boundary conditions of the problem are specified as follows:

On the top and bottom surfaces the transverse loads are given by

$$\begin{bmatrix}\tau_{13m} & \sigma_{3m}\end{bmatrix} = \begin{bmatrix}0 & \bar{q}_{3m}^{\pm}\end{bmatrix} \quad \text{on } x_3 = \pm 1 \tag{15}$$

where $\bar{q}_{3m}^{\pm} = \bar{q}_{zm}^{\pm}/(Q \in^3)$, such that $\bar{q}_{3m}^{+} = C_W(\bar{u}_{3(m+1)} - \bar{u}_{3m})$ when m=1-(N_l-1), $\bar{q}_{3m}^{-} = C_W(\bar{u}_{3m} - \bar{u}_{3(m-1)})$ when m=2-N_l, $\bar{q}_{3N_l}^{\pm} = -\bar{q}_3$ and $\bar{q}_{31}^{-} = K_W \bar{u}_{31}$, in which $\bar{q}_3^{+} = \bar{q}_z^{+}/\left(Q \in^3\right)$ and $(C_W,\ K_W) = (c_w,\ k_w)\left[L^4/\left(Qh^3\right)\right]$.

At the edges (x_1=0 and x_1=L_x/L), the boundary conditions are

$$\sigma_{1m} = u_{3m} = 0 \tag{16}$$

2.3 Asymptotic expansion

Because Eqs. (10)-(14) contain terms involving only even powers of $\in$, the authors asymptotically expand the field variables in the powers $\in^2$, as given by

$$f = f^{(0)}(x_1,\ x_3) + \in^2 f^{(1)}(x_1,\ x_3) + \in^4 f^{(2)}(x_1,\ x_3) + \cdots \tag{17}$$

Substituting Eq. (17) into Eqs. (10)-(14) and collecting the coefficients of equal powers of $\in$, the authors obtain the recursive sets of the basic equations of each individual GS for various order problems as follows:

For the $\in^0$-order problem,

$$u_{3m}^{(0)},_3 = 0 \tag{18}$$

$$u_{1m}^{(0)},_3 = -u_{3m}^{(0)},_1 \tag{19}$$

$$\left[\left(1-\bar{\mu}_1 \partial_{11}\right)\tau_{13m}^{(0)}\right],_3 = -\tilde{Q}_{11}\, u_{1m}^{(0)},_{11}, \tag{20}$$

$$\left[\left(1-\bar{\mu}_1 \partial_{11}\right)\sigma_{3m}^{(0)}\right],_3 = -\left[\left(1-\bar{\mu}_1 \partial_{11}\right)\tau_{13m}^{(0)}\right],_1 \tag{21}$$

$$\left(1-\bar{\mu}_1 \partial_{11}\right)\sigma_{1m}^{(0)} = \tilde{Q}_{11}\, u_{1m}^{(0)},_1 \tag{22}$$

For the $\in^{2k}$-order problem (k=1, 2, 3, etc.),

$$\begin{aligned} u_{3m}^{(k)},_3 = &-\tilde{c}_{13}\, u_{1m}^{(k-1)},_1 + \tilde{c}_{33}^{-1}\left(1-\bar{\mu}_1 \partial_{11}\right)\sigma_{3m}^{(k-2)} \\ &-\left(\tilde{c}_{33}^{-1}\, \bar{\mu}_2 \partial_{33}\right) \sigma_{3m}^{(k-3)} \end{aligned} \tag{23}$$

$$\begin{aligned} u_{1m}^{(k)},_3 = &-u_{3m}^{(k)},_1 + \tilde{c}_{55}^{-1}\left(1-\bar{\mu}_1 \partial_{11}\right)\tau_{13m}^{(k-1)} \\ &-\tilde{c}_{55}^{-1}\left(\bar{\mu}_2 \partial_{33}\right)\tau_{13m}^{(k-2)} \end{aligned} \tag{24}$$

$$\begin{aligned} \left[\left(1-\bar{\mu}_1 \partial_{11}\right)\tau_{13m}^{(k)}\right],_3 = &-\tilde{Q}_{11}\, u_{1m}^{(k)},_{11} + \left(\bar{\mu}_2 \partial_{333}\right)\tau_{13m}^{(k-1)} \\ &-\tilde{c}_{13}\left[\left(1-\bar{\mu}_1 \partial_{11}\right)\sigma_{3m}^{(k-1)}\right],_1 + \tilde{c}_{13}\left[\left(\bar{\mu}_2 \partial_{33}\right)\sigma_{3m}^{(k-2)}\right],_1 \end{aligned} \tag{25}$$

$$\left[\left(1-\bar{\mu}_1 \partial_{11}\right)\sigma_{3m}^{(k)}\right],_3 = -\left[\left(1-\bar{\mu}_1 \partial_{11}\right)\tau_{13m}^{(k)}\right],_1 \tag{26}$$

$$\begin{aligned} \left(1-\bar{\mu}_1 \partial_{11}\right)\sigma_{1m}^{(k)} = &\ \tilde{Q}_{11}\, u_{1m}^{(k)},_1 + \left(\bar{\mu}_2 \partial_{33}\right)\sigma_{1m}^{(k-1)} \\ &+ \tilde{c}_{13}\left(1-\bar{\mu}_1 \partial_{11}\right)\sigma_{3m}^{(k-1)} - \tilde{c}_{13}\left(\bar{\mu}_2 \partial_{33}\right)\sigma_{3m}^{(k-2)} \end{aligned} \tag{27}$$

The boundary conditions of each individual GS for various order problems are specified as follows:

On the lateral surface the transverse loads are Order $\in^0$,

$$\begin{bmatrix}\tau_{13m}^{(0)} & \sigma_{3m}^{(0)}\end{bmatrix} = \begin{bmatrix}0 & \left(\bar{q}_{3m}^{\pm}\right)^{(0)}\end{bmatrix} \quad \text{on} \quad x_3 = \pm 1 \tag{28a}$$

Order $\in^{2k}$ (k =1, 2, 3, etc.),

$$\begin{bmatrix}\tau_{13m}^{(k)} & \sigma_{3m}^{(k)}\end{bmatrix} = \begin{bmatrix}0 & \left(\bar{q}_{3m}^{\pm}\right)^{(k)}\end{bmatrix} \quad \text{on} \quad x_3 = \pm 1 \tag{28b}$$

Along the edges (x_1=0 and x_1 = L_x/L), the boundary conditions are given, as follows: order $\in^{2k}$ (k =0, 1, 2, 3, etc.),

$$\sigma_{1m}^{(k)} = u_{3m}^{(k)} = 0 \tag{29}$$

2.4 Governing equations for various order problems

2.4.1 The leading order problems

The sets of GEs for various order problems can be carried out by integrating the corresponding basic equations through the thickness direction. The authors thus integrate Eqs. (18) and (19) to obtain

$$u_{3m}^{(0)} = u_{3m}^{0}\,(x_1) \tag{30}$$

$$u_{1m}^{(k)} = u_{1m}^{k}\left(x_1\right) - x_3\, u_{3m}^{k},_1 + \varphi_{1m}^{(k)}\left(x_1, x_3\right) \tag{31}$$

where u_{3m}^{0} and u_{1m}^{0} represent the displacement components on the mid-plane of each individual GS, and these also refer to the Kirchhoff-Love type displacement model in CPT.

With the lateral boundary conditions on x_3=-1 given in Eq. (28a), the authors then proceed to integrate Eqs. (20) and (21), which yields

$$\left(1-\bar{\mu}_1\partial_{11}\right)\tau_{13m}^{(0)} = \int_{-1}^{x_3}\left[-\tilde{Q}_{11}\left(u_{1m}^{0},_{11} - \eta\, u_{3m}^{0},_{111}\right)\right]d\eta \tag{32}$$

$$\begin{aligned}&\left(1-\bar{\mu}_1\,\partial_{11}\right)\left[\sigma_{3m}^{(0)} - \left(\bar{q}_{3m}^{-}\right)^{(0)}\right]\\ &= -\int_{-1}^{x_3}(x_3-\eta)\left[-\tilde{Q}_{11}\left(u_{1m}^{0},_{111} - \eta\, u_{3m}^{0},_{1111}\right)\right]d\eta\end{aligned} \tag{33}$$

Imposing the remaining lateral boundary conditions on x_3=1 given in Eq. (28b) on Eqs. (32) and (33), the authors obtain

$$-\tilde{A}_{11}\, u_{1m}^{0},_{11} + \tilde{B}_{11}\, u_{3m}^{0},_{111} = 0 \tag{34}$$

$$-\tilde{B}_{11}\, u_{1m}^{0},_{111} + \tilde{D}_{11}\, u_{3m}^{0},_{1111} = \left(1-\bar{\mu}_1\,\partial_{11}\right)\left[\left(\bar{q}_{3m}^{+}\right)^{(0)} - \left(\bar{q}_{3m}^{-}\right)^{(0)}\right] \tag{35}$$

where $\tilde{A}_{ij} = \int_{-1}^{1}\tilde{Q}_{ij}\,dx_3$, $\tilde{B}_{ij} = \int_{-1}^{1}x_3\,\tilde{Q}_{ij}\,dx_3$, and $\tilde{D}_{ij} = \int_{-1}^{1}x_3^2\,\tilde{Q}_{ij}\,dx_3$.

In this article, the edge boundary conditions of the infinite multiple-GS system in the *x* direction are considered to be fully simply-supported edges. After the asymptotic process, the authors thus obtain the edge conditions for the leading order problem, as follows:

$$\begin{gathered}u_{3m}^{0} = 0\ ,\quad N_{1m}^{(0)} = 0 \text{ and } \quad M_{1m}^{(0)} = 0\ ,\\ \text{at } \ x_1 = 0 \ \text{ and } \ x_1 = L_x/L\end{gathered} \tag{36}$$

where $N_{1m}^{(0)} = \int_{-1}^{1}\sigma_{1m}^{(0)}\,dx_3$, $M_{1m}^{(0)} = \int_{-1}^{1}x_3\,\sigma_{1m}^{(0)}\,dx_3$.

By introducing the tractional normal foces $(\bar{q}_{3m}^{+})^{(0)}$ and $(\bar{q}_{3m}^{-})^{(0)}$ on the top and bottom surfaces of the m^{th}-GS, and then assembling the GEs of each individual GS to form the GEs of the multiple GS system, the resulting GEs for the single-, double-, and triple-GS system are expressed in detail as follows:

For a single GS system,

$$\begin{bmatrix}K_{11} & K_{13}\\ K_{13} & \left(K_{33}+K_{33}^{*}\right)\end{bmatrix}\begin{Bmatrix}u_{11}^{0}\\ u_{31}^{0}\end{Bmatrix} = \begin{Bmatrix}0\\ -\left(1-\bar{\mu}_1\,\partial_{11}\right)\bar{q}_3\end{Bmatrix} \tag{37}$$

where $K_{11} = -\tilde{A}_{11}\partial_{11}$, $K_{13} = \tilde{B}_{11}\partial_{111}$, $K_{31} = -\tilde{B}_{11}\partial_{111}$, $K_{33} = \tilde{D}_{11}\partial_{1111}$, and $K_{33}^{*} = \left(1-\bar{\mu}_1\partial_{11}\right)K_w$.

For a double GS system,

$$\begin{bmatrix}K_{11} & K_{13} & 0 & 0\\ K_{13} & \left(K_{33}+K_{33}^{*}+D_{33}\right) & 0 & -D_{33}\\ 0 & 0 & K_{11} & K_{13}\\ 0 & -D_{33} & K_{13} & \left(K_{33}+D_{33}\right)\end{bmatrix}\begin{Bmatrix}u_{11}^{0}\\ u_{31}^{0}\\ u_{12}^{0}\\ u_{32}^{0}\end{Bmatrix} = \begin{Bmatrix}0\\ 0\\ 0\\ -\left(1-\bar{\mu}_1\partial_{11}\right)\bar{q}_3\end{Bmatrix} \tag{38}$$

where $D_{33} = \left(1-\bar{\mu}_1\partial_{11}\right)C_w$.

For a triple GS system,

$$\begin{bmatrix}K_{11} & K_{13} & 0 & 0 & 0 & 0\\ K_{13} & \left(K_{33}+K_{33}^{*}+D_{33}\right) & 0 & -D_{33} & 0 & 0\\ 0 & 0 & K_{11} & K_{13} & 0 & 0\\ 0 & -D_{33} & K_{13} & \left(K_{33}+2D_{33}\right) & 0 & -D_{33}\\ 0 & 0 & 0 & 0 & K_{11} & K_{13}\\ 0 & 0 & 0 & -D_{33} & K_{13} & \left(K_{33}+D_{33}\right)\end{bmatrix}\begin{Bmatrix}u_{11}^{0}\\ u_{31}^{0}\\ u_{12}^{0}\\ u_{32}^{0}\\ u_{13}^{0}\\ u_{33}^{0}\end{Bmatrix} = \begin{Bmatrix}0\\ 0\\ 0\\ 0\\ 0\\ -\left(1-\bar{\mu}_1\,\partial_{11}\right)\bar{q}_3\end{Bmatrix},\ etc. \tag{39}$$

It is noted that Eqs. (37)-(39) are exactly the same as the nonlocal multiple CPT system equations, which have thus been derived as first-order approximations of the nonlocal plane strain elasticity theory. The solutions for Eqs. (37)-(39) must be supplemented with the edge boundary conditions given in Eq. (29) to constitute a well-posed boundary value problem. Once the variables of u_{1m}^{0} and u_{3m}^{0} (m=1-N_l) are determined, the leading-order displacement solutions through the thickness direction of each individual GS are given by Eqs. (30) and (31), and the transverse shear and normal stresses are given by Eqs. (32) and (33). Then, the in-surface stresses are given by Eq. (27).

2.4.2 Higher-order problems

Proceeding to order $\in^{2k}$ (k=1, 2, 3, …) and following a similar process as that performed in the $\in^{0}$ -order problem, the authors readily obtain

$$u_{3m}^{(k)} = u_{3m}^{k}\left(x_1\right) + \varphi_{3m}^{(k)}\left(x_1, x_3\right) \tag{40}$$

$$u_{1m}^{(k)} = u_{1m}^{k}\left(x_1\right) - x_3\, u_{3m}^{k},_1 + \varphi_{1m}^{(k)}\left(x_1, x_3\right) \tag{41}$$

$$\left(1-\bar{\mu}_1\,\partial_{11}\right)\tau_{13m}^{(k)}=\int_{-1}^{x_3}-\tilde{Q}_{11}\left(u_{1m}^{k},_{11}-\eta\,u_{3m}^{k},_{111}\right)d\eta-f_{1m}^{(k)} \quad (42)$$

$$\begin{aligned}&\left(1-\bar{\mu}_1\,\partial_{11}\right)\left[\,\sigma_{3m}^{(k)}-\left(\bar{q}_{3m}^{-}\right)^{(k)}\right]\\&=-\int_{-1}^{x_3}\left(x_3-\eta\right)\left[-\tilde{Q}_{11}\left(u_{1m}^{k},_{11}-\eta\,u_{3m}^{k},_{111}\right)\right],_1 d\eta-f_{3m}^{(k)}\end{aligned} \quad (43)$$

where

$$\varphi_{3m}^{(k)}=\int_0^{x_3}\Big[-\tilde{c}_{13}\,u_{1m}^{(k-1)},_1+\tilde{c}_{33}^{-1}\left(1-\bar{\mu}_1\,\partial_{11}\right)\sigma_{3m}^{(k-2)} -\left(\tilde{c}_{33}^{-1}\,\bar{\mu}_2\,\partial_{33}\right)\sigma_{3m}^{(k-3)}\Big]\,d\eta$$

$$\varphi_{1m}^{(k)}=\int_0^{x_3}\Big[-\varphi_{3m}^{(k)},_1+\tilde{c}_{55}^{-1}\left(1-\bar{\mu}_1\,\partial_{11}\right)\tau_{13m}^{(k-1)} -\tilde{c}_{55}^{-1}\left(\bar{\mu}_2\,\partial_{33}\right)\tau_{13m}^{(k-2)}\Big]\,d\eta$$

$$f_{1m}^{(k)}=\int_{-1}^{x_3}\Big\{\tilde{Q}_{11}\,\varphi_{1m}^{(k)},_{11}+\tilde{c}_{13}\left[\left(1-\bar{\mu}_1\,\partial_{11}\right)\sigma_{3m}^{(k-1)}\right],_1 -\tilde{c}_{13}\left[\left(\bar{\mu}_2\,\partial_{33}\right)\sigma_{3m}^{(k-2)}\right],_1-\left(\bar{\mu}_2\,\partial_{333}\right)\tau_{13m}^{(k-1)}\Big\}\,d\eta$$

$$f_{3m}^{(k)}\left(x_1,\,x_3\right)=-\int_{-1}^{x_3}f_{1m}^{(k)},_1\,d\eta\,.$$

u_{3m}^{k} and u_{1m}^{0} represent the k^{th}-order modifications to the variables of the mid-plane displacement components of the m^{th}-GS. By imposing the associated lateral boundary conditions (Eq. (28b)) on Eqs. (42) and (43), the authors again obtain the multiple CPT governing equations, and the nonhomogeneous terms can be calculated using the lower-order solution. The resulting equations are obtained, as follows:

$$K_{11}\,u_{1m}^{k}+K_{13}\,u_{3m}^{k}=f_{1m}^{(k)}\left(1\right) \quad (44)$$

$$\begin{aligned}K_{31}\,u_{1m}^{k}+K_{33}\,u_{3m}^{k}&=\left(1-\bar{\mu}_1\,\partial_{11}\right)\left[\left(\bar{q}_{3m}^{+}\right)^{(k)}-\left(\bar{q}_{3m}^{-}\right)^{(k)}\right]\\&\quad+f_{3m}^{(k)}\left(1\right)+f_{1m}^{(k)}\left(1\right),_1\end{aligned} \quad (45)$$

The edge conditions for the higher-order problems ar given, as follows:

$$u_{3m}^{k}=0\;,\quad N_{1m}^{(k)}=0\quad\text{and}\quad M_{1m}^{(k)}=0\;,\quad \text{at}\;\; x_1=0\;\;\text{and}\;\; x_1=L_x/L \quad (46)$$

where $N_1^{(k)}=\int_{-1}^{1}\sigma_1^{(k)}\,dx_3$, $M_1^{(k)}=\int_{-1}^{1}x_3\,\sigma_1^{(k)}\,dx_3$.

After an assembly process, the GEs of the single-, double-, and triple-GS systems are expressed in detail as follows:

For a single GS system,

$$\begin{bmatrix}K_{11} & K_{13}\\ K_{13} & \left(K_{33}+K_{33}^{*}\right)\end{bmatrix}\begin{Bmatrix}u_{11}^{k}\\ u_{31}^{k}\end{Bmatrix}=\begin{Bmatrix}f_{11}^{(k)}\left(1\right)\\ f_{31}^{(k)}\left(1\right)+f_{11}^{(k)}\left(1\right),_1\end{Bmatrix}. \quad (47)$$

For a double GS system,

$$\begin{bmatrix}K_{11} & K_{13} & 0 & 0\\ K_{13} & \left(K_{33}+K_{33}^{*}+D_{33}\right) & 0 & -D_{33}\\ 0 & 0 & K_{11} & K_{13}\\ 0 & -D_{33} & K_{13} & \left(K_{33}+D_{33}\right)\end{bmatrix}\begin{Bmatrix}u_{11}^{k}\\ u_{31}^{k}\\ u_{12}^{k}\\ u_{32}^{k}\end{Bmatrix}=\begin{Bmatrix}f_{11}^{(k)}\left(1\right)\\ f_{31}^{(k)}\left(1\right)+f_{11}^{(k)}\left(1\right),_1\\ f_{12}^{(k)}\left(1\right)\\ f_{32}^{(k)}\left(1\right)+f_{12}^{(k)}\left(1\right),_1\end{Bmatrix} \quad (48)$$

For a triple GS system,

$$\begin{bmatrix}K_{11} & K_{13} & 0 & 0 & 0 & 0\\ K_{13} & \left(K_{33}+K_{33}^{*}+D_{33}\right) & 0 & -D_{33} & 0 & 0\\ 0 & 0 & K_{11} & K_{13} & 0 & 0\\ 0 & -D_{33} & K_{13} & \left(K_{33}+2D_{33}\right) & 0 & -D_{33}\\ 0 & 0 & 0 & 0 & K_{11} & K_{13}\\ 0 & 0 & 0 & -D_{33} & K_{13} & \left(K_{33}+D_{33}\right)\end{bmatrix}\begin{Bmatrix}u_{11}^{k}\\ u_{31}^{k}\\ u_{12}^{k}\\ u_{32}^{k}\\ u_{13}^{k}\\ u_{33}^{k}\end{Bmatrix}=\begin{Bmatrix}f_{11}^{(k)}\left(1\right)\\ f_{31}^{(k)}\left(1\right)+f_{11}^{(k)}\left(1\right),_1\\ f_{12}^{(k)}\left(1\right)\\ f_{32}^{(k)}\left(1\right)+f_{12}^{(k)}\left(1\right),_1\\ f_{13}^{(k)}\left(1\right)\\ f_{33}^{(k)}\left(1\right)+f_{13}^{(k)}\left(1\right),_1\end{Bmatrix},\ etc. \quad (49)$$

The higher-order modifications for the mid-plane displacement components of the m^{th}-GS of the single-, double-, and triple-GS systems (u_{1m}^{k}, u_{2m}^{k} and u_{3m}^{k}) can be obtained by solving Eqs. (47), (48), and (49), respectively, combined with the edge conditions given in Eqs. (46). Once these are determined, the higher-order modifications of the displacement components of each individual GS are given by Eqs. (40) and (41), the transverse stresses are given by Eqs. (42) and (43) and the in-surface stresses are given by Eq. (28).

Equations (37)-(39) and (47)-(49) show that the differential operators among the various order problems remain identical, and the nonhomogeneous terms of higher-order problems can be calculated from the lower-order solution. The solution process of the leading-order problem can be repeatedly applied to the higher-order problems. The present asymptotic solutions can thus be determined order-by-order in a hierarchical and consistent manner.

3. Applications

3.1 Leading order solutions

The bending problem of simply-supported, single-, double-, and triple-GS systems are studied by using the single Fourier series expansion method, in which the displacement and stress components are expanded as single Fourier series functions in the x direction. For the current issue, the governing equations of the leading-order problem can thus be solved by letting

$$u_{1m}^{0}\left(x_1\right)=\sum_{\hat{n}=1}^{\infty} \tilde{u}_{1m\hat{n}}^{0} \cos\tilde{n}x_1 \tag{50}$$

$$u_{3m}^{0}\left(x_1\right)=\sum_{\hat{n}=1}^{\infty} \tilde{u}_{3m\hat{n}}^{0} \sin\tilde{n}x_1 \tag{51}$$

where $\tilde{n}=\hat{n}\pi L/L_x$, and $\hat{n}$ denotes the half-wave numbers and is a positive integer.

According to Eqs. (30)-(33) and (27), the other field variables should be also the forms of single Fourier series functions, such that the simply-supported edge conditions are satisfied, and these are given as

$$\left[u_{1m}^{(0)} \quad \tau_{13m}^{(0)}\right]=\sum_{\hat{n}=1}^{\infty}\left[\tilde{u}_{1m\hat{n}}^{(0)}\left(x_3\right) \quad \tilde{\tau}_{13m\hat{n}}^{(0)}\left(x_3\right)\right]\cos\tilde{n}x_1 \tag{52}$$

$$\begin{aligned}&\left[u_{3m}^{(0)} \quad \sigma_{1m}^{(0)} \quad \sigma_{3m}^{(0)}\right]\\ &=\sum_{\hat{n}=1}^{\infty}\left[\tilde{u}_{3m\hat{n}}^{(0)}\left(x_3\right) \quad \tilde{\sigma}_{1m\hat{n}}^{(0)}\left(x_3\right) \quad \tilde{\sigma}_{3m\hat{n}}^{(0)}\left(x_3\right)\right]\sin\tilde{n}x_1\end{aligned} \tag{53}$$

For brevity, the summation sign will not be shown in the following derivation.

Substituting Eqs. (50)-(53) into Eqs. (37)-(39) gives the GEs of the single-, double, and triple-GS systems, as follows:

For a single GS system,

$$\begin{bmatrix} k_{11} & k_{13} \\ k_{31} & \left(k_{33}+k_{33}^{*}\right)\end{bmatrix}\begin{Bmatrix}\tilde{u}_{11\hat{n}}^{0}\\ u_{31\hat{n}}^{0}\end{Bmatrix}=\begin{Bmatrix}0\\ -\left(1+\tilde{n}^2\bar{\mu}_1\right)\tilde{q}_{3\hat{n}}\end{Bmatrix} \tag{54}$$

where $k_{11}=\tilde{n}^2\widetilde{A_{11}}$, $k_{13}=k_{31}=-\tilde{n}^3\widetilde{B_{11}}$, $k_{33}=\tilde{n}^4\widetilde{D_{11}}$, $k_{33}^{*}=(1+\tilde{n}^2\widetilde{\mu_1})K_w$, and the applied external load on the top surface of the GS system is expressed as $\bar{q}_3^{+}\left(x_1\right)=\tilde{q}_{3\hat{n}}\sin\tilde{n}x_1$.

For a double GS system,

$$\begin{aligned}&\begin{bmatrix} k_{11} & k_{13} & 0 & 0\\ k_{31} & \left(k_{33}+k_{33}^{*}+d_{33}\right) & 0 & -d_{33}\\ 0 & 0 & k_{11} & k_{13}\\ 0 & -d_{33} & k_{13} & \left(k_{33}+d_{33}\right)\end{bmatrix}\begin{Bmatrix}\tilde{u}_{11\hat{n}}^{0}\\ \tilde{u}_{31\hat{n}}^{0}\\ \tilde{u}_{12\hat{n}}^{0}\\ \tilde{u}_{32\hat{n}}^{0}\end{Bmatrix}\\ &=\begin{Bmatrix}0\\0\\0\\ -\left(1+\hat{n}^2\bar{\mu}_1\right)\tilde{q}_{3\hat{n}}\end{Bmatrix}\end{aligned} \tag{55}$$

where $d_{33}=\left(1+\tilde{n}^2\bar{\mu}_1\right)C_w$.

For a triple GS system,

$$\begin{bmatrix} k_{11} & k_{13} & 0 & 0 & 0 & 0\\ k_{31} & \left(k_{33}+k_{33}^{*}+d_{33}\right) & 0 & -d_{33} & 0 & 0\\ 0 & 0 & k_{11} & k_{13} & 0 & 0\\ 0 & -d_{33} & k_{31} & \left(k_{33}+2d_{33}\right) & 0 & -d_{33}\\ 0 & 0 & 0 & 0 & k_{11} & k_{13}\\ 0 & 0 & 0 & -d_{33} & k_{13} & \left(k_{33}+d_{33}\right)\end{bmatrix} \tag{56}$$

$$\begin{Bmatrix}\tilde{u}_{11\hat{n}}^{0}\\ \tilde{u}_{31\hat{n}}^{0}\\ \tilde{u}_{12\hat{n}}^{0}\\ \tilde{u}_{32\hat{n}}^{0}\\ \tilde{u}_{13\hat{n}}^{0}\\ \tilde{u}_{33\hat{n}}^{0}\end{Bmatrix}=\begin{Bmatrix}0\\0\\0\\0\\0\\ -\left(1+\tilde{n}^2\bar{\mu}_1\right)\tilde{q}_{3\hat{n}}\end{Bmatrix},\ \text{etc.}$$

After the above GEs of a multiple GS system are solved, the through-thickness distributions of the various field variables of each individual GS for the leading-order problem can then be obtained, as follows:

$$\tilde{u}_{3m\hat{n}}^{(0)}=\tilde{u}_{3m\hat{n}}^{0} \tag{57}$$

$$\tilde{u}_{1m\hat{n}}^{(0)}=\tilde{u}_{1m\hat{n}}^{0}-x_3\,\tilde{n}\,\tilde{u}_{3m\hat{n}}^{0} \tag{58}$$

$$\left(1+\tilde{n}^2\bar{\mu}_1\right)\tilde{\tau}_{13m\hat{n}}^{(0)}=\int_{-1}^{x_3}\left[-\tilde{Q}_{11}\left(-\tilde{n}^2\tilde{u}_{1m\hat{n}}^{0}+\eta\,\tilde{n}^3\tilde{u}_{3m\hat{n}}^{0}\right)\right]d\eta, \tag{59}$$

$$\begin{aligned}&\left(1+\tilde{n}^2\bar{\mu}_1\right)\left[\tilde{\sigma}_{3m\hat{n}}^{(0)}-\left(\bar{q}_{3m\hat{n}}^{-}\right)^{(0)}\right]\\ &=-\int_{-1}^{x_3}\left(x_3-\eta\right)\left[-\tilde{Q}_{11}\left(\tilde{n}^3\tilde{u}_{1m\hat{n}}^{0}-\eta\,\tilde{n}^4\,\tilde{u}_{3m\hat{n}}^{0}\right)\right]d\eta,\end{aligned} \tag{60}$$

$$\left(1+\tilde{n}^2\bar{\mu}_1\right)\tilde{\sigma}_{1m\hat{n}}^{(0)}=-\tilde{n}\,\tilde{Q}_{11}\,\tilde{u}_{1m\hat{n}}^{(0)} \tag{61}$$

3.2 Higher-order modifications

$$\left[f_{1m\hat{n}}^{(k)} \quad \varphi_{1m\hat{n}}^{(k)}\right]=\sum_{\hat{n}=1}^{\infty}\left[\tilde{f}_{1m\hat{n}}^{(k)}\left(x_3\right) \quad \tilde{\varphi}_{1m\hat{n}}^{(k)}\left(x_3\right)\right]\cos\tilde{n}x_1, \tag{62}$$

$$\left[f_{3m}^{(k)} \quad \varphi_{3m}^{(k)}\right]=\sum_{\hat{n}=1}^{\infty}\left[\tilde{f}_{3m\hat{n}}^{(k)}\left(x_3\right) \quad \tilde{\varphi}_{3m\hat{n}}^{(k)}\left(x_3\right)\right]\sin\tilde{n}x_1 \tag{63}$$

where $\tilde{f}_{im\hat{n}}^{(k)}$ and $\tilde{\phi}_{im\hat{n}}^{(k)}$ $\left(i=1 \text{ and } 3\right)$ are the relevant coefficients.

The governing equations of the higher-order problems can be solved by letting

$$u_{1m\hat{n}}^{k}\left(x_1\right)=\sum_{\hat{n}=1}^{\infty} \tilde{u}_{1m\hat{n}}^{k} \cos\tilde{n}x_1 \tag{64}$$

$$u_{3m}^{k}\left(x_1\right)=\sum_{\hat{n}=1}^{\infty} \tilde{u}_{3m\hat{n}}^{k} \sin\tilde{n}x_1 \tag{65}$$

The other field variables of the k^{th}-order problems are also expanded in the form of single Fourier series functions, such that the simply-supported edge conditions are satisfied, and these are given as

$$\left[u_{1m}^{(k)} \quad \tau_{13m}^{(k)}\right]=\sum_{\hat{n}=1}^{\infty}\left[\tilde{u}_{1m\hat{n}}^{(k)}\left(x_3\right) \quad \tilde{\tau}_{13m\hat{n}}^{(k)}\left(x_3\right)\right]\cos\tilde{n}x_1 \tag{66}$$

$$\begin{aligned}&\left[u_{3m}^{(k)} \quad \sigma_{1m}^{(k)} \quad \sigma_{3m}^{(k)}\right]\\&=\sum_{\hat{n}=1}^{\infty}\left[\tilde{u}_{3m\hat{n}}^{(k)}\left(x_3\right) \quad \tilde{\sigma}_{1m\hat{n}}^{(k)}\left(x_3\right) \quad \tilde{\sigma}_{3m\hat{n}}^{(k)}\left(x_3\right)\right]\sin\tilde{n}x_1\end{aligned} \tag{67}$$

The summation sign will not be shown in the following derivation for brevity.

The resulting GEs of a multiple GS system are thus obtained by substituting Eqs. (64)-(67) into Eqs. (47)-(49), and they are given as:

For a single GS system,

$$\begin{bmatrix} k_{11} & k_{13} \\ k_{13} & \left(k_{33}+k_{33}^{*}\right) \end{bmatrix}\begin{Bmatrix} \tilde{u}_{11\hat{n}}^{k} \\ \tilde{u}_{31\hat{n}}^{k} \end{Bmatrix}=\begin{Bmatrix} \tilde{f}_{11\hat{n}}^{(k)}(1) \\ \tilde{f}_{31\hat{n}}^{(k)}(1)-\tilde{n}\,\tilde{f}_{11\hat{n}}^{(k)}(1) \end{Bmatrix}. \tag{68}$$

For a double GS system,

$$\begin{aligned}&\begin{bmatrix} k_{11} & k_{13} & 0 & 0 \\ k_{13} & \left(k_{33}+k_{33}^{*}+d_{33}\right) & 0 & -d_{33} \\ 0 & 0 & k_{11} & k_{13} \\ 0 & -d_{33} & k_{13} & \left(k_{33}+d_{33}\right) \end{bmatrix}\begin{Bmatrix} \tilde{u}_{11\hat{n}}^{k} \\ \tilde{u}_{31\hat{n}}^{k} \\ \tilde{u}_{12\hat{n}}^{k} \\ \tilde{u}_{32\hat{n}}^{k} \end{Bmatrix}\\&=\begin{Bmatrix} \tilde{f}_{11\hat{n}}^{(k)}(1) \\ \tilde{f}_{31\hat{n}}^{(k)}(1)-\tilde{n}\,\tilde{f}_{11\hat{n}}^{(k)}(1) \\ \tilde{f}_{12\hat{n}}^{(k)}(1) \\ \tilde{f}_{32\hat{n}}^{(k)}(1)-\tilde{n}\,\tilde{f}_{12\hat{n}}^{(k)}(1) \end{Bmatrix}\end{aligned} \tag{69}$$

For a triple GS system,

$$\begin{aligned}&\begin{bmatrix} k_{11} & k_{13} & 0 & 0 & 0 & 0 \\ k_{31} & \left(k_{33}+k_{33}^{*}+d_{33}\right) & 0 & -d_{33} & 0 & 0 \\ 0 & 0 & k_{11} & k_{13} & 0 & 0 \\ 0 & -d_{33} & k_{13} & \left(k_{33}+2d_{33}\right) & 0 & -d_{33} \\ 0 & 0 & 0 & 0 & k_{11} & k_{13} \\ 0 & 0 & 0 & -d_{33} & k_{13} & \left(k_{33}+d_{33}\right) \end{bmatrix}\\&\begin{Bmatrix} \tilde{u}_{11\hat{n}}^{k} \\ \tilde{u}_{31\hat{n}}^{k} \\ \tilde{u}_{12\hat{n}}^{k} \\ \tilde{u}_{32\hat{n}}^{k} \\ \tilde{u}_{13\hat{n}}^{k} \\ \tilde{u}_{33\hat{n}}^{k} \end{Bmatrix}=\begin{Bmatrix} \tilde{f}_{11\hat{n}}^{(k)}(1) \\ \tilde{f}_{31\hat{n}}^{(k)}(1)-\tilde{n}\,\tilde{f}_{11\hat{n}}^{(k)}(1) \\ \tilde{f}_{12\hat{n}}^{(k)}(1) \\ \tilde{f}_{32\hat{n}}^{(k)}(1)-\tilde{n}\,\tilde{f}_{12\hat{n}}^{(k)}(1) \\ \tilde{f}_{13\hat{n}}^{(k)}(1) \\ \tilde{f}_{33\hat{n}}^{(k)}(1)-\tilde{n}\,\tilde{f}_{13\hat{n}}^{(k)}(1) \end{Bmatrix},\ etc.\end{aligned} \tag{70}$$

After the above GEs of a multiple GS system are solved, the through-thickness distributions of various field variables of the k^{th}-order modifications can be obtained, as follows:

$$\tilde{u}_{3m\hat{n}}^{(k)}=\tilde{u}_{3m\hat{n}}^{k}+\tilde{\varphi}_{3m\hat{n}}^{(k)} \tag{71}$$

$$\tilde{u}_{1m\hat{n}}^{(k)}=\tilde{u}_{1m\hat{n}}^{k}-x_3\,\tilde{n}\,u_{3\hat{m}\hat{n}}^{k}+\tilde{\varphi}_{1m\hat{n}}^{(k)} \tag{72}$$

$$\left(1+\tilde{n}^2\bar{\mu}_1\right)\tilde{\tau}_{13mn}^{(k)}=\int_{-1}^{x_3}-\tilde{Q}_{11}\left(-\tilde{n}^2\tilde{u}_{1m\hat{n}}^{k}+\eta\,\tilde{n}^3\tilde{u}_{3m\hat{n}}^{k}\right)d\eta-\tilde{f}_{1m\hat{n}}^{(k)} \tag{73}$$

$$\begin{aligned}&\left(1+\tilde{n}^2\bar{\mu}_1\right)\left[\tilde{\sigma}_{3m\hat{n}}^{(k)}-\left(\bar{q}_{3m\hat{n}}^{-}\right)^{(k)}\right]\\&=-\int_{-1}^{x_3}\left(x_3-\eta\right)\left[-\tilde{Q}_{11}\left(\tilde{n}^3\tilde{u}_{1m\hat{n}}^{k}-\eta\,\tilde{n}^4\tilde{u}_{3m\hat{n}}^{k}\right)\right]d\eta-\tilde{f}_{3m\hat{n}}^{(k)}\end{aligned} \tag{74}$$

$$\begin{aligned}\left(1+\tilde{n}^2\bar{\mu}_1\right)\tilde{\sigma}_{1m\hat{n}}^{(k)}=&-\tilde{n}\,\tilde{Q}_{11}\,\tilde{u}_{1m\hat{n}}^{(k)}+\bar{\mu}_2\,\tilde{\sigma}_{1m\hat{n}}^{(k-1)},_{33}\\&+\tilde{c}_{13}\left(1+\tilde{n}^2\bar{\mu}_1\right)\tilde{\sigma}_{3m\hat{n}}^{(k-1)}-\tilde{c}_{13}\,\bar{\mu}_2\,\tilde{\sigma}_{3m\hat{n}}^{(k-2)},_{33}\end{aligned} \tag{75}$$

In this work the contributions of the nonlocal parameter (μ) in the length and thickness directions were separated in this dimensionless formulation as $\overline{\mu_1}$ and $\overline{\mu_2}$, respectively, because the thickness dimension is much less than the length dimension for each individual GS. In the following numerical examples, the authors thus let $\overline{\mu_1}=\overline{\mu_2}$, the corresponding relations of which in a dimensional form are $\mu_1=\mu$ and $\mu_2=\mu\in^2$, to reasonably equalize their contributions to the mechanical behaviors of these multiple GS systems.

4. Illustrative examples

4.1 Single-layered orthotropic macroplates

A benchmark problem with regard to the static analysis of simply-supported, orthotropic macroplates under cylindrical bending-type sinusoidally distributed loads was investigated by Pagano (1969). For comparison purposes, Pagano's solutions can be used to validate the accuracy and convergence of the asymptotic nonlocal plane strain theory in the case of μ=0.

Table 1 shows the dimensionless displacement and stress components induced in single-layered orthotropic macroplates in cylindrical bending, in which the sinusoidally distributed loads are applied on the top surface of the macroplate with $\hat{n}=1$, i.e. $\bar{q}_z(x)=\sin(\pi x/L_x)$. The material properties used in the cases are E_L/E_T= 25 and 50; G_{LT}/E_T=0.5; G_{TT}/E_T=0.2; $\upsilon_{LT}=\upsilon_{TT}=0.25$, in which the subscripts L and T denote the directions parallel and perpendicular to the fiber direction, respectively. The geometric parameters of the plate are H/L_x=0.15 and 0.25.

For comparison purposes, a set of dimensionless forms of stress and displacement variables is defined as follows:

$$\begin{aligned}&\bar{u}_x=u_xE_T/\left(q_0H\right),\ \bar{u}_z=100u_zH^3E_T/\left(q_0L_x^4\right),\\&\bar{\sigma}_x=\sigma_x/q_0,\ \bar{\tau}_{xz}=\tau_{xz}/q_0,\ \bar{\sigma}_z=\sigma_z/q_0\end{aligned} \tag{76a-e}$$

It can be seen in Table 1 that the asymptotic solutions converge rapidly. The convergent solutions are obtained at the $\in^6$-order level in the cases of thick plates (H/L_x=0.15),

Table 1 Dimensionless displacement and stress components induced in single-layer orthotropic macroplates under cylindrical bending-type sinusoidally distributed loads

H/L_x	E_L/E_T	Theories	$\bar{u}_x(0,h)$	$\bar{u}_z\left(\frac{L_x}{2},0\right)$	$\bar{\sigma}_x\left(\frac{L_x}{2},h\right)$	$\bar{\tau}_{xz}(0,0)$	$\bar{\sigma}_z\left(\frac{L_x}{2},h\right)$
0.15	25	Present $\in^0$	2.2877	0.4915	27.0190	3.1831	1.0000
		Present $\in^2$	2.6803	1.0361	31.9687	3.0373	1.0000
		Present $\in^4$	2.6705	1.0272	31.8534	3.0565	1.0000
		Present $\in^6$	2.6707	1.0280	31.8553	3.0539	1.0000
		Present $\in^8$	2.6711	1.0279	31.8598	3.0543	1.0000
		Exact 3D (Pagano 1969)	NA	1.0279	31.8585	3.0542	1.0000
		TSDT (Sayyad and Ghugal 2016)	2.7218	1.0253	32.2959	3.2321 (3.0178)	NA
		HSDT (Reddy 1984)	2.7066	1.0315	31.9659	3.1415 (3.0374)	NA
		FSDT (Mindlin 1951)	2.2877	0.9475	27.0190	2.1221 (3.1831)	NA
		CPT	2.2877	0.4915	27.0190	NA	NA
0.15	50	Present $\in^0$	1.1453	0.2461	27.0190	3.1831	1.0000
		Present $\in^2$	1.5538	0.7919	36.9686	2.8900	1.0000
		Present $\in^4$	1.5103	0.7758	35.9442	2.9713	1.0000
		Present $\in^6$	1.5189	0.7793	36.1469	2.9488	1.0000
		Present $\in^8$	1.5184	0.7783	36.1335	2.9549	1.0000
		Exact 3D (Pagano 1969)	NA	0.7786	36.1252	2.9536	1.0000
		TSDT (Sayyad and Ghugal 2016)	1.5799	0.7723	37.4132	3.1806 (2.8575)	NA
		HSDT (Reddy 1984)	1.5588	0.7791	36.7732	3.1010 (2.8958)	NA
		FSDT (Mindlin 1951)	1.1453	0.7020	27.0190	2.1221 (3.1831)	NA
		CPT	1.1453	0.2461	27.0190	NA	NA
0.25	25	Present $\in^0$	0.4941	0.4915	9.7268	1.9099	1.0000
		Present $\in^2$	0.7297	2.0042	14.6766	1.6669	1.0000
		Present $\in^4$	0.7134	1.9354	14.3562	1.7330	1.0000
		Present $\in^6$	0.7142	1.9538	14.3712	1.7221	1.0000
		Present $\in^8$	0.7191	1.9472	14.4679	1.7348	1.0000
		Exact 3D (Pagano 1969)	NA	1.9420	14.4091	1.7314	1.0000
		TSDT (Sayyad and Ghugal 2016)	0.7523	1.9233	14.9471	1.8836 (1.6374)	NA
		HSDT (Reddy 1984)	0.7397	1.9574	14.5613	1.8420 (1.6725)	NA
		FSDT (Mindlin 1951)	0.4941	1.7580	9,7268	1.2732 (1.9099)	NA
		CPT	0.4941	0.4915	9.7268	NA	NA
0.25	50	Present $\in^0$	0.2474	0.2461	9.7268	1.9099	1.0000
		Present $\in^2$	0.4925	1.7623	19.6765	1.4214	1.0000
		Present $\in^4$	0.4201	1.6377	16.8307	1.7979	1.0000
		Present $\in^6$	0.4599	1.7128	18.3953	1.5075	1.0000
		Present $\in^8$	0.4526	1.6577	18.1070	1.7283	1.0000
		Exact 3D (Pagano 1969)	NA	1.6813	17.9270	1.6332	1.0000
		TSDT (Sayyad and Ghugal 2016)	0.4988	1.6194	19.7404	1.8033 (1.5388)	NA
		HSDT (Reddy 1984)	0.4846	1.6618	19.0534	1.7790 (1.5283)	NA
		FSDT (Mindlin 1951)	0.2474	1.5126	9.7268	1.2732 (1.9099)	NA
		CPT	0.2474	0.2461	9.7268	NA	NA

The solutions in the parentheses are obtained using the stress equilibrium equations.

and the $\in^8$-order level in the cases of very thick plates (H/L_x=0.25) as compared with the 3D exact solutions obtained by Pagano (1969). The convergent asymptotic solutions also closely agree with those obtained by Sayyad and Ghugal (2016) using the TSDT and by Reddy (1984) using the refined higher-order shear deformation theory (HSDT). The deviation between the current $\in^6$-order solutions and the 3D exact solutions decreases when the plate becomes thinner and also when the values of E_L/E_T become smaller. The solutions for the transverse stress components in the parentheses were obtained using the stress equilibrium equations, which were used to improve these solutions obtained using the constitutive equations for the PVD-based plate theories, such as the TSDT, HSDT, etc. Because the current formulation is based on the RMVT, in which the displacement and transverse stress variables are the primary variables, their accuracy is at the same level and much better than that obtained using the PVD-based theories, in which the transverse stress variables are the secondary variables and are usually obtained using the determined displacement variables and the corresponding constitutive equations.

Table 2 The convergent ($\in^8$ –order) solutions for the stress and displacement components of simply-supported, single-, double-, and triple-GS systems in cylindrical bending under sinusoidal distributed loads

No. layers (N_l)	Variables	K_w = 50			K_w = 100			K_w = 200		
		$\mu=0$ nm^2	$\mu=1$ nm^2	$\mu=2$ nm^2	$\mu=0$ nm^2	$\mu=1$ nm^2	$\mu=2$ nm^2	$\mu=0$ nm^2	$\mu=1$ nm^2	$\mu=2$ nm^2
N_l=1	$\bar{u}_{x1}(0,h)$	2737.6	2885.5	3021.8	1915	1986.1	2049.7	1195.7	1223.0	1246.8
	$\bar{u}_{z1}(L_x/2,0)$	-6.8692	-7.2404	-7.5827	-4.8063	-4.9852	-5.1451	-3.0028	-3.0717	-3.1316
	$\bar{\tau}_{xz1}(0,0)$	-8.0149	-7.6892	-7.3889	-5.6080	-5.2941	-5.0136	-3.5036	-3.2620	-3.0516
	$\bar{\sigma}_{z1}(L_x/2,h)$	-1.0000	-1.0000	-1.0000	-1.0000	-1.0000	-1.0000	-1.0000	-1.0000	-1.0000
N_l=2	$\bar{u}_{x1}(0,h)$	1223.7	1339.5	1450.9	927.0	1001.2	1071.1	624.1	665.0	702.8
	$\bar{u}_{z1}(L_x/2,0)$	-3.0705	-3.3612	-3.6407	-2.3266	-2.5131	-2.6885	-1.5672	-1.6703	-1.7652
	$\bar{\tau}_{xz1}(0,0)$	-3.5826	-3.5695	-3.5476	-2.7146	-2.6689	-2.6198	-1.8286	-1.7738	-1.7201
	$\bar{\sigma}_{z1}(L_x/2,h)$	-0.4470	-0.4642	-0.4801	-0.4841	-0.5041	-0.5225	-0.5219	-0.5438	-0.5637
	$\bar{u}_{x2}(0,h)$	2649.8	2820.6	2982.7	2471.4	2609.7	2738.3	2289.3	2400.1	2501.4
	$\bar{u}_{z2}(L_x/2,0)$	-6.6468	-7.0754	-7.4822	-6.1997	-6.5468	-6.8697	-5.7433	-6.0214	-6.2757
	$\bar{\tau}_{xz2}(0,0)$	-7.7507	-7.5093	-7.2865	-7.2294	-6.9483	-6.6901	-6.6972	-6.3908	-6.1117
	$\bar{\sigma}_{z2}(L_x/2,h)$	-0.9986	-0.9986	-0.9987	-0.9985	-0.9986	-0.9986	-0.9986	-0.9986	-0.9987
N_l=3	$\bar{u}_{x1}(0,h)$	551.4	625.3	698.8	424.8	476.3	526.7	291.0	322.5	352.7
	$\bar{u}_{z1}(L_x/2,0)$	-1.3836	-1.5691	-1.7536	-1.0662	-1.1955	-1.3220	-0.7309	-0.8098	-0.8859
	$\bar{\tau}_{xz1}(0,0)$	-1.6144	-1.6664	-1.7087	-1.2441	-1.2696	-1.2882	-0.8528	-0.8600	-0.8633
	$\bar{\sigma}_{z1}(L_x/2,h)$	-0.2014	-0.2167	-0.2313	-0.2218	-0.2398	-0.2569	-0.2434	-0.2637	-0.2829
	$\bar{u}_{x2}(0,h)$	1194.1	1316.8	1436.6	1132.6	1241.4	1346.5	1067.7	1163.7	1255.4
	$\bar{u}_{z2}(L_x/2,0)$	-2.9952	-3.3031	-3.6039	-2.8412	-3.1144	-3.3779	-2.6785	-2.9195	-3.1496
	$\bar{\tau}_{xz2}(0,0)$	-3.4927	-3.5057	-3.5096	-3.3131	-3.3054	-3.2896	-3.1235	-3.0986	-3.0673
	$\bar{\sigma}_{z2}(L_x/2,h)$	-0.4499	-0.4661	-0.4809	-0.4575	-0.4749	-0.4909	-0.4656	-0.4841	-0.5011
	$\bar{u}_{x3}(0,h)$	2631.6	2806.0	2973.1	2594.5	2759.0	2915.0	2555.4	2710.4	2856.3
	$\bar{u}_{z3}(L_x/2,0)$	-6.6002	-7.0378	-7.4571	-6.5075	-6.9200	-7.3116	-6.4096	-6.7984	-7.1645
	$\bar{\tau}_{xz3}(0,0)$	-7.6942	-7.4673	-7.2599	-7.5863	-7.3424	-7.1183	-7.4722	-7.2135	-6.9753
	$\bar{\sigma}_{z3}(L_x/2,h)$	-0.9983	-0.9983	-0.9984	-0.9982	-0.9983	-0.9983	-0.9982	-0.9983	-0.9983

Figure 2 shows the current asymptotic solutions for various orders with regard to the through-thickness distributions of the stress and displacement components induced in an infinitely long, and thick macroplate under sinosoidal distributed loads, in which E_L/E_T =25, and H/L_x=0.25. It can be seen in Fig. 2 that the asymptotic solutions for the through-thickness distributions of stress and displacement components converge rapidly and that the convergent solutions were yielded at the $\in^4$ – order level. The current asymptotic solutions for the transverse stress components exactly satisfied the traction stress conditions on the top and bottom surfaces of the plate. The results also show that the through-thickness distributions of the in-plane displecement and in-plane stress components appear to be higher-order polynomial function distributions, rather than the linear function distributions assumed in the CST and FSDT, *a priori*. The CPT and FSDT thus might not be suitable for the analysis of thick macroplates due to the obvious discrepancies between the true through-thickness distributions of the in-plane displacements and their corresponding kinematic assumptions in CST and FSDT, which are planes that remain planes after deformation.

4.2 Multiple GS systems

In this section, we examine the static behavior of simply-supported, single-, double-, and triple-GS systems subjected to cylindrical bending-type sinosoidally-distributed mechanical loads, i.e., $\bar{q}_z(x) = \sin(\pi x/L_x)$. The material properties and geometric parameters of each individual GS are given as E=1.02 TPa, $\upsilon = 0.16$, C_w=100, L_x=10 nm, and H=0.34 nm. Table 2 shows the convergent solutions (i.e. $\in^8$ -order ones) for the nonlocal displacement and stress components at the crucial positions of these GSs with different values of the nonlocal parameters (μ) and the foundation parameter (K_w). It can be seen in Table 2 that the nonlocal displacement and stress components increase when the nonlocal parameter becomes greater, while these components decrease when either the number of GSs in the multiple-GS system or the foundation stiffness increase.

Figure 3 shows the through-thickness distributions of various nonlocal field variables induced in the triple-GS systems, in which C_w=K_w=50 and μ =0, 1 and 2 nm^2. It can be seen in Fig. 3 that the nonlocal displacement components are always larger than their corresponding local components,

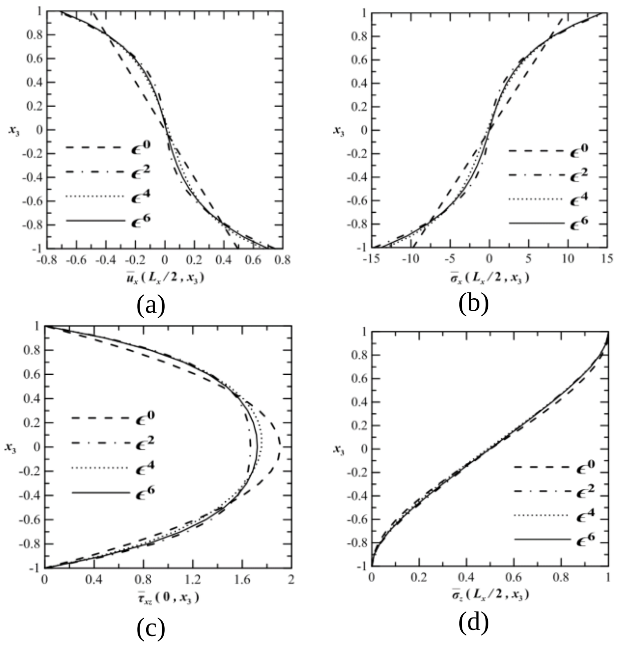

Fig. 2 Through-thickness distributions of assorted primary variables induced in a single-layered orthotropic macroplate under sinusoidally-distributed loads

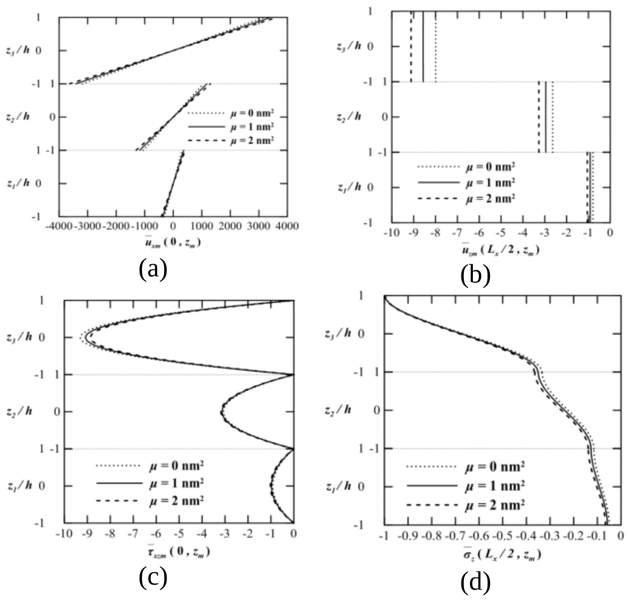

Fig. 3 Variations in the through-thickness distributions of assorted primary variables induced in a triple-GS system with different values of the nonlocal parameter

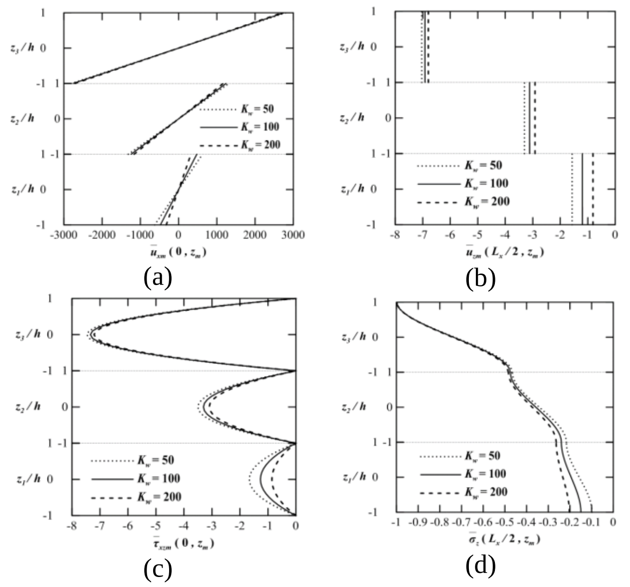

Fig. 4 Variations in the through-thickness distributions of assorted primary variables induced in a triple-GS system with different values of K_w

and that these will increase when the value of the nonlocal parameter becomes greater, which indicates that the small length scale effect will soften the triple-GS system. The influence with regard to the variations in the through-thickness distributions of out-of-plane displacement components with an increasing nonlocal parameter is much more significant than those of other variables, such as the in-plane displacement and transverse stress components. In this formulation, Winkler models with C_w are introduced to simulate the interaction effect between adjacent GSs, such that the in- and out-of-plane displacement components are discontinuous at the interfaces between adjacent GSs, while the transverse shear and normal stress components are continuous in these locations.

Figure 4 shows the variations in the through-thickness distributions of various nonlocal field variables induced in the triple GS systems with the stiffness parameters of the foundation, in which C_w=100, μ =1 nm^2. and K_w=50 , 100 and 200. It can be seen in Figs. 4(a) and 4(b) that the current solutions of displacement components of the triple-GS system at the interfaces between adjacent GSs are discontinuous, which is different from those induced at the interfaces between adjacent layers for the macroscale laminated composite structures, in which the perfect bonding assumptions were assumed *in priori*. The results also show that variations in the through-thickness distributions of various nonlocal field variables induced in each individual GS with the stiffness parameters of the foundation are in the following order: the topmost GS (m=3) < the middle GS (m=2) < the bottommost GS (m=1), in which the symbol "<" meams less significant. Because the external loads are applied on the top surface of the topmost GS, the maximum values of various field variables induced in the triple-GS system occur at the topmost GS. In this case (L_x/H=29.4 and μ =1 nm^2), $(u_{x3})_{max}:(u_{z3})_{max}$ = 9.354x10^{-19} q_0:1.755x10$^{-17}q_0$, which means the maximum value of the out-of-plane displacement component is about 18.76 times that of the in-plane displacement component, and $(\tau_{xz3})_{max}:(\sigma_{z3})_{max}$ =7.467q_0:q_0, which means the maximum value of the transver shear component is about 7.47 times that of the transverse normal stress component.

Figure 5 shows the variations in the through-thickness distributions of various nonlocal field variables induced in the triple-GS systems with the Winkler's parameter between adjacent GSs, in which K_w =200, μ =1nm^2, and C_w=50,100 and 200. It can be seen in Figs. 5(c) and 5(d) that the current solutions of the transverse shear stresses at the top and bottom surfaces of each individual GS are zeros due to the fact that the traction shear forces at those places

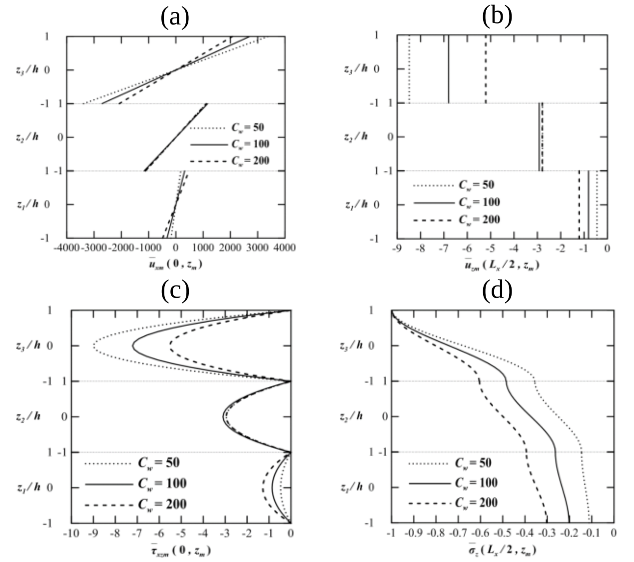

Fig. 5 Variations in the through-thickness distributions of assorted primary variables induced in a triple-GS system with different values of C_w

are free. The solutions of the transverse normal stresses at the top surface of the topmost GS and at the bottom surface of the bottommost GS are identical to the applied external load and the spring force of the foundation, respectively.

The solutions of the transverse normal stresses at the interfaces between adjacent GSs are continuous and are identical to the spring forces of the Winkler model considered. The results also show variations in the through-thickness distributions of various nonlocal field variables induced in the each individual GS with the Winkler parameters between adjacent GSs are in the following order: the topmost GS (m=3) > the middle GS (m=2) > the bottommost GS (m=1), in which the symbol ">" meams more significant, the trend of which is exactly the opposite of that shown in Fig. 4. In this case, $(u_{x3})_{max}:(u_{z3})_{max}$ = $1.128\text{x}10^{-18}q_0$: $2.117\text{x}10^{-17}q_0$, which means the maximumvalue of the out-of-plane displacement component is about 18.77 times that of the in-plane displacement component, and $(\tau_{xz3})_{max}:(\sigma_{z3})_{max}=9.01q_0:q_0$, which means the maximum value of the transverse shear component is about 9.01 times that of transverse normal stress component.

5. Concluding remarks

In this article, the authors first reformulate the local plane strain elasticity theory in order to conduct cylindrical bending analysis of simply-supported, infinitely long, single-, double-, and multiple-GS systems using the perturbation method, in which the ENCR is used to account for the small length scale effect. After applying the perturbation approach, the nonlocal multiple CPT is derived as the leading-order approximation of the nonlocal plane strain elasticity theory, and the governing equations for the higher-order problems remain the same as those of the nonlocal multiple CPT, although with different nonhomogeneous terms, which can be determined by the lower-order solutions. The current nonlocal asymptotic theory can also be reduced to its local counterpart by letting the nonlocal parameter (i.e., μ =0) be zero.

The current 3D asymptotic theory for multiple-GS systems is superior to 2D nonlocal advanced and refined plate theories available in the literature. In the former no kinematic and kinetic assumptions must be made in advance and the accuracy of lower-order solutions can be improved in a hierarchical and consistent manner, while in the latter a specific kinematic or kinetic assumption needs to be made *in priori* and the accuracy of their solutions cannot be enhanced without reformulation.

The validity of the current 3D asymptotic theory depends upon the selection of the nonlocal parameter μ, which can be determined from experiments or by matching dispersion curves of plane waves with those of atomic lattice dynamics.

In the numerical examples, the convergent asymptotic solutions are obtained at the ϵ^6- and ϵ^8-order levels for the cases of H/L_x=0.15 and 0.25, respectively, and these convergent solutions closely agree with Pagano's 3D solutions available in the literature. It is noted that the nonlocal displacement and stress components increase when the nonlocal parameter becomes greater, while these components decrease when either the number of GSs in the multiple-GS system or the foundation stiffness increase. Moreover, some benchmark solutions for simply-supported, single-, double-, and triple-GS systems subjected to the cylindrical bending-type loads are presented. These solutions can serve as a standard for assessing the performance of various 2D nonlocal advanced and refined multiple plate theories.

Acknowledgment

This work was supported by the Ministry of Science and Technology of the Republic of China through Grant MOST 106-2221-E-006-036-MY3.

References

Aghababaei, R., Reddy, J. N. (2009), "Nonlocal third-order shear deformation plate theory with application to bending and vibration of plates", *J. Sound Vib.,* **326**(1-2), 277-289. https://doi.org/10.1016/j.jsv.2009.04.044.

Anjomshoa, A., Shahidi, A.R., Hassani, B. and Jomehzadeh, E. (2014), "Finite element buckling analysis of multi-layered graphene sheets on elastic substrate based on nonlocal elasticity theory", *Appl. Math. Modell.*, **38**, 5934-3955. https://doi.org/10.1016/j.apm.2014.03.036

Arani, A.G., Shiravand, A., Rahi, M. and Kolahchi, R. (2012), "Nonlocal vibration of coupled DLGS systems embedded on visco-Pasternak foundation", *Physica B*, **407**(21), 4123-4131. https://doi.org/10.1016/j.physb.2012.06.035.

Bakshi, S.R., Lahiri, D. and Agarwal, A. (2010), "Carbon nanotube reinforced metal matrix composites-a review", *Int. Mater. Rev.*, **55**(1), 41-64. https://doi.org/10.1179/095066009x12572530170543.

Belkorissat, I., Houari, M.S.A., Tounsi, A., Bedia, E.A.A. and Mahmoud, S.R. (2015), "On vibration properties of functionally graded nano-plate using a new nonlocal refined four variable model", *Steel Compos. Struct.*, **18**(4), 1063-1081.

https://doi.org/10.12989/scs.2015.18.4.1063.

Bessaim, A., Houari, M.S.A., Bernard, F. and Tounsi, A. (2015), "A nonlocal quasi-3D trigonometric plate model for free vibration behavior of micro/nanoscale plates", *Struct. Eng. Mech*., **56**(2), 223-240. https://doi.org/10.12989/sem.2015.56.2.223.

Besseghier, A., Houari, M.S.A., Tounsi, A. and Mahmoud, S.R. (2017), "Free vibration analysis of embedded nanosize FG plates using a new nonlocal trigonometric shear deformation theory", *Smart Struct. Syst.* **19**(6), 601-614. https://doi.org/10.12989/sss.2017.19.6.601.

Bounouara, F., Benrahou, K.H., Belkorissat, I. and Tounsi, A. (2016), "A nonlocal zeroth-order shear deformation theory for free vibration of functionally graded nanoscale plates resting on elastic foundation", *Steel Compos. Struct*., **20**(2), 227-249. https://doi.org/10.12989/sss.2016.20.2.227.

Eringen, A.C. (1972), "Nonlocal polar elastic continua", *Int. J. Eng. Sci.*, **10**(1), 1-16. https://doi.org/10.1016/0020-7225(72)90070-5.

Eringen, A.C. (2002), *Nonlocal Continuum Field Theories*, Springer-Verlag, New York.

Eringen, A.C., Edelen, D.G.B. (1972), "On nonlocal elasticity", *Int. J. Eng. Sci.*, **10**(3), 233-248. https://doi.org/10.1016/0020-7225(72)90039-0.

Fahsi, B., Kaci, A., Tounsi, A., Bedia, E.A.A. (2012), "A four variable refined plate theory for nonlinear cylindrical bending analysis of functionally graded plates under thermomechanical loadings", *J. Mech. Sci. Technol*., **26**(12), 4073-4079. https://doi.org/10.1007/s12206-012-0907-4

Iijima, S. (1991), "Helical microtubules of graphitic carbon", *Nature*, **354**, 56-58.

Jomehzadeh, E. and Saidi, A.R. (2011), "Decoupling the nonlocal elasticity equations for three dimensional vibration analysis of nano-plates", *Compos. Struct*., **93**, 1015-1020. https://doi.org/10.1016/j.compstruct.2010.06.017.

Karličić, D., Kozić, P., Adhikari, S., Cajić, M., Murmu, T. and Lazarević, M. (2015), "Nonlocal mass-nanosensor model based on the damped vibration of single-layer graphene sheet influenced by in-plane magnetic field", *Int. J. Mech. Sci.*, **96-97**, 132-142. https://doi.org/10.1016/j.ijmecsci.2015.03.014.

Karličić, D., Kozić, P. and Pavlović, R. (2016), "Nonlocal vibration and stability of a multiple-nanobeam system coupled by the Winkler elastic medium", *Appl. Math. Modell*. **40**(2), 1599-1614. https://doi.org/10.1016/j.apm.2015.06.036.

Khaniki, H.B. (2018), "On vibrations of nanobeam systems", *Int. J. Eng. Sci*. **124**, 85-103. https://doi.org/10.1016/j.ijengsci.2017.12.010.

Khetir, H., Bouiadjra, M.B., Houari, M.S.A., Tounsi, A. and Mahmoud, S.R. (2017), "A new nonlocal trigonometric shear deformation theory for thermal buckling analysis of embedded nanosize FG plates", *Struct. Eng. Mech*., **64**(4), 391-402. https://doi.org/10.12989/sem.2017.64.4.391.

Kippenberg, T.J. and Vahala, K.J. (2007), "Cavity opto-mechanics", *Opt. Express* **15**(25), 17172-17205. https://doi.org/10.1364/OE.15.017172.

Kuila, T, Bose, S., Khanra, P., Mishra, A.K., Kim, N.H. and Lee, J.H. (2011), "Recent advances in graphene-based biosensors", *Biosensors Bioelectronics* **26**(12), 4637-4648. https://doi.org/10.1016/j.bios.2011.05.039.

Metcalfe, M. (2014), "Applications of cavity optomechanics", *Appl. Phys. Rev.*, **1**, 031105 (18 pages). https://doi.org/10.1063/1.4896029.

Mindlin, R.D. (1951), "Influence of rotatory inertia and shear on flexural motions of isotropic, elastic plates", *J. Appl. Mech*., **44**, 669-676.

Murmu, T. and Adhikari, S. (2010), "Nonlocal transverse vibration of double-nanobeam-systems", *J. Appl. Phys.* **108**, 083514 (9 pages). https://doi.org/10.1063/1.3496627.

Naderi, A. and Saidi, A.R. (2014), "Nonlocal postbuckling analysis of graphene sheets in a nonlinear polymer medium", *Int. J. Eng. Sci*., **81**, 49-65. https://doi.org/10.1016/j.ijengsci.2014.04.004.

Naderi, A. and Saidi, A.R. (2014), "Modified nonlocal Mindlin plate theory for buckling analysis of nanoplates", *J. Nanomech. Micromech.*, **4**(4), A4013015 (8 pages). https://doi.org/10.1061/(ASCE)NM.2153-5477.0000068.

Navazi, H.M. and Haddadpour, H. (2008), "Nonlinear cylindrical bending analysis of shear deformable functionally graded plates under different loadings using analytical methods", *Int. J. Mech. Sci*., **50**(12), 1650-1657. https://doi.org/10.1016/j.ijmecsci.2008.08.010.

Nayfeh, A.H. (1993), *Introduction to Perturbation Techniques*, John Wiley & Sons, Inc., New York.

Novoselov, K.S., Geim, A.K., Morozov, S.V., Jiang, D., Zhang, Y., Dubonos, S.V., Grigorieva, I.V., Firsov, A.A. (2004), "Electric field effect in atomically thin carbon films", *Science*, **306**, 666-669. https://doi.org/10.1126/science.1102896.

Pagano, N.J. (1969), "Exact solutions for composite laminates in cylindrical bending", *J. Compos. Mater*., **3**, 398-411. https://doi.org/10.1177/002199836900300304.

Park, J. and Lee, S.Y. (2003), "A new exponential plate theory for laminated composites under cylindrical bending", *Trans. Japan Soc. Aero. Space Sci*., **46**(152), 89-95. https://doi.org/10.2322/tjsass.46.89.

Pradhan, S.C., Phadikar, J.K. (2009), "Nonlocal elasticity theory for vibration of nanoplates", *J. Sound Vib*., **325**, 206-223. https://doi.org/10.1016/j.jsv.2009.03.007.

Pumera, M., Ambrosi, A., Bonanni, A., Chng, E.L.K. and Poh, H.L. (2010), "Graphene for electrochemical sensing and biosensing", *Trends Analyt. Chem*. **29**(9), 954-965. https://doi.org/10.1016/j.trac.2010.05.011.

Rajabi, K. and Hosseini-Hashemi, Sh. (2017a), "On the application of viscoelastic orthotropic double-nanoplates systems as nanoscale mass-sensors via the generalized Hooke's law for viscoelastic materials and Erigen's nonlocal elasticity theory", *Compos. Struct*. **180**, 105-115. https://doi.org/10.1016/j.compstruct.2017.07.085.

Rajabi, K. and Hosseini-Hashemi, Sh. (2017b), "A new nanoscale mass sensor based on a bilayer graphene nanoribbon: The effect of interlayer shear on frequencies shift", *Comput. Mater. Sci*., **126**, 468-473. https://doi.org/10.1016/j.commatsci.2016.08.052.

Reddy, J.N. (1984), "A simple higher order theory for laminated composite plates", *J. Appl. Mech*., **51**(4), 745-752. https://doi.org/10.11115/1.3167719.

Reddy, J.N. (2010), "Nonlocal nonlinear formulations for bending of classical and shear deformation theories of beams and plates", *Int. J. Eng. Sci.,* **48**, 1507-1518. https://doi.org/10.1016/j.ijengsci.2010.09.020.

Sayyad, A.S., Ghugal, Y.M. (2016), "Cylindrical bending of multilayered composite laminates and sandwiches", *Adv. Aircraft Spacecraft Sci*., **3**(2), 113-148. https://doi.org/10.12989/aas.2016.3.2.113.

Sayyad, A.S., Ghumare, S.M. and Sasane, S.T. (2014), "Cylindrical bending of orthotropic plate strip based on nth-order plate theory", *J. Mater. Eng. Struct.*, **1**, 47-57.

She, G.L., Yuan, F.G. and Ren, Y.R. (2017), "Research on nonlinear bending behaviors of FGM infinite cylindrical shallow shells resting on elastic foundations in thermal environments", *Compos. Struct.*, **170**, 111-121. https://doi.org/10.1016/j.compstruct.2017.03.010.

Sobhy, M. (2017), "Hygro-thermo-mechanical vibration and buckling of exponentially graded nanoplates resting on elastic foundations via nonlocal elasticity theory", *Struct. Eng. Mech*., **63**(3), 401-415. https://doi.org/10.12989/sem.2017.63.3.401.

Thai, H.T. (2012), "A nonlocal beam theory for bending, buckling, and vibration of nanobeams", *Int. J. Eng. Sci.,* **52**, 56-64. https://doi.org/10.1016/j.ijengsci.2011.11.011.

Thai, H.T., Vo, T.P. (2012), "A nonlocal sinusoidal shear deformation beam theory with application to bending, buckling, and vibration of nanobeams", *Int. J. Eng. Sci.,* **54**, 58-66.

https://doi.org/10.1016/j.ijengsci.2012.01.009.
Thai, H.T., Vo, T.P., Nguyen, T.K. and Lee, J. (2014), "A nonlocal sinusoidal plate model for micro/nanoscale plates", *Proc. Inst. Mech. Eng., Part C: J. Mech. Eng. Sci.,* **228**, 2652-2660. https://doi.org/10.1177/0954406214521391.
Wu, C.P. and Chen, Y.J. (2019), "Cylindrical bending vibration of multiple graphene sheet systems embedded in an elastic medium", *Int. J. Struct. Stab. Dyn*., **19**(3), 1950035 (27 pages). https://doi.org/10.1142/S0219455419500354.
Yazid, M., Heireche, H., Tounsi, A., Bousahla, A.A. and Houari, M.S.A. (2018), "A novel nonlocal refined plate theory for stability response of orthotropic single-layer graphene sheet resting on elastic medium", *Smart Struct. Syst.* **21**(1), 15-25. https://doi.org/10.12989/sss.2018.21.1.015.
Yengejeh, S.I., Kazemi, S.A. and Ochsner, A. (2017), "Carbon nanotubes as reinforcement in composites: A review of the analytical, numerical and experimental approaches", *Comput. Mater. Sci*., **136**, 85-101. https://doi.org/10.1016/j.commatsci.2017.04.023.

CC